Study of the Interactions of Model Polymer Surface with Cold Plasmas. II. Degradation Rate Versus Pressure and Gas Flow Rate

M. K. SHI and F. CLOUET*

Institut Charles Sadron, 6 rue Boussingault, 67083 Strasbourg, France

SYNOPSIS

This work deals with the influence of pressure, gas flow rate, and gas mixture on the etching rates of polymer model molecules such as hexatriacontane ($C_{36}H_{74}$) and octadecyl octadecanoate (OOD) treated in an oxygen or argon plasma. Mass spectrometry and optical emission spectroscopy have been used to monitor the formation and evolution of the fragments coming from chain breaking in terms of their concentration and emission intensity, respectively. It was demonstrated that pressure and gas flow rate are two important parameters in the interaction of cold plasmas and of polymer surfaces. The results obtained can be explained by combined effects such as electron energy and its density, residence time, "quenching effect," as well as chemical reactions. © 1992 John Wiley & Sons, Inc.

INTRODUCTION

Of the many studies devoted to the polymer degradation induced by low-temperature plasmas,[1-11] only a few have studied the influence of pressure and gas flow rate.[2-5] Compared to the applied power influence, pressure and gas flow rate will modify not only the electron energy and its density but also the residence time and the diffusion rate of the active species.[12,13] Yasuda et al.[2] reported for the first time the effect of gas flow rate on the etching rates of polymer fibers. It was assumed that at low gas flow rates, it is the mass flow rate that is the degradation rate-determining factor while at high flow rates, the discharge power becomes the rate-determining factor. Lerner and Wydeven[3] studied the etching of polybutadiene isomers exposed to oxygen afterglow; they observed that even at constant O-atom concentration, the etching rates decrease almost linearly with increasing O-atom flow rate from 2 to 10 $cm^3_{(STP)}$/min. This behavior was explained as a result of the more efficient elimination of the reactive intermediates (˙OH, for example) from the reaction

sites with increasing gas flow rate. Yasuda et al.[4] observed that the influence of pressure in an He plasma has no effect on the degradation of poly(oxymethylene). Hartney et al.[5] reported that the etching of novolac polymers in an RIE reactor shows a maximum value.

In our first study,[14] we investigated the effect of the treatment time and the applied power on the degradation of polymer model molecules: $C_{36}H_{74}$ and OOD treated by O_2 and Ar plasmas and the formation of volatile fragments stemming from the surface reactions. The principal results are: (1) the degradation rates increase linearly with the treatment time and the applied power for both oxygen and argon plasmas; (2) the introduction of one ester group on $C_{36}H_{74}$ increases the degradation rate, especially in an oxygen plasma; (3) CO, CO_2, H_2O, and H_2 are the main degradation products in an oxygen plasma, and H_2 is the main one detected by mass spectrometry in an argon plasma; (4) the concentrations of CO and CO_2 reach a maximum faster than those of H_2O and H_2; (5) a steady state is established after 2 min; and (6) a discharge power increase induced a modification of the gas phase composition. Based on these observations, a mechanism was proposed to explain the above phenomena.

In this study, we describe the influence of gas flow rate, pressure, and gas mixture on the degradation rate and the formation, evolution, and emission intensity of the volatile compounds.

EXPERIMENTAL

Apparatus

The plasma apparatus and the treatment process have been described in details elsewhere.[14] Briefly, the plasma is created in a cylindrical reactor, the cover of which forms the cathode capacitively coupled to a 13.56-MHz energy generator. The anode on which are placed the samples is a 15-cm disk whose temperature is kept constant thanks to water circulation. The volume of the reactor is about 1500 cm^3. Pressure and gas flow rate are measured with a Baratron pressure transducer and mass flow meter, respectively. The pressure can be adjusted by a nitrogen flow introduced between the plasma chamber and the pump.

The variation of the plasma gas phase composition was monitored by mass spectrometry. The quadrupole mass spectrometer VG instrument (SXP 300) is connected to the reactor output. To take into account the molecules that can come from the reactor walls, sampling was done with and without a sample. In Figure 1(a) and 1(b) are shown the ratios $[C_x]/[C_0]_{O2}$ or $[C_x]/[C_0]_{Ar}$ for prominent species in the gas phase without plasma, with plasma but without sample and at last with plasma and sample ($C_{36}H_{74}$). In an oxygen glow discharge, the concentration of oxygen molecules decreases more and more for these three experiments, while those of the prominent species increases strongly, especially when a sample is present. The increase of H_2, H_2O, CO, and CO_2 in the discharge without sample can be attributed to the contaminants coming from the reactor walls. The same evolution is observed in the case of an argon plasma, but the variation is very small. It is known that the mass spectrum of a complex molecule is composed of different fragments. To take this effect into account, we have listed in Table I the main fragmentation peaks for H_2, H_2O, CO, and CO_2. The parent peak represents at least 80% of the total fragments in all cases. The calculated difference between mass peak intensities without and with a sample indicates the relative concentrations of the effluents coming from the sample surface. Typical operating conditions of the mass spectrometer were given in the first study.[14]

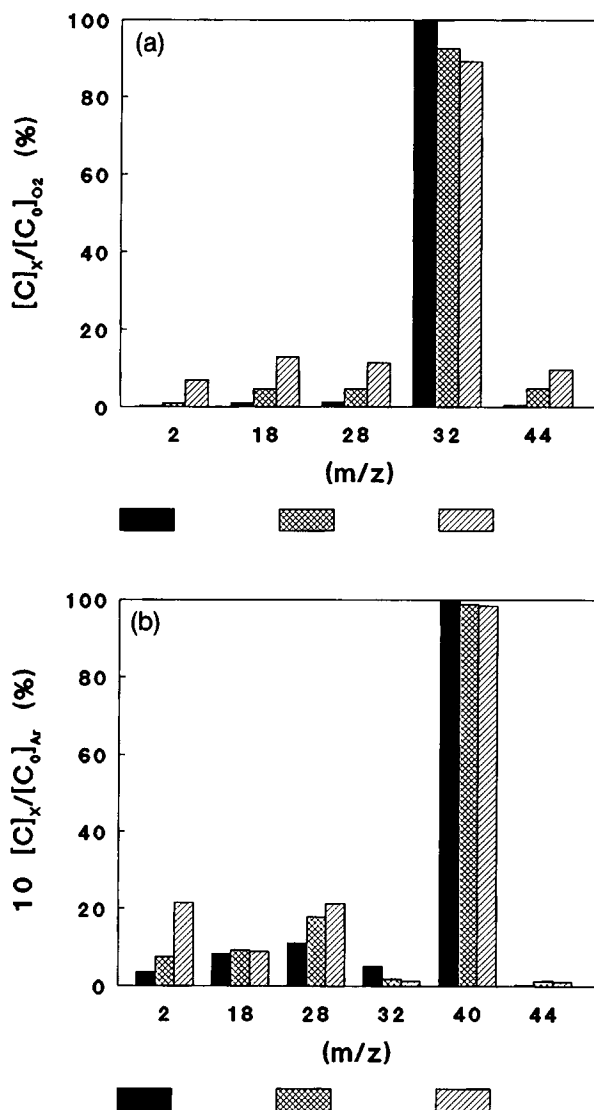Plasma emission is collected through a quartz window, looking radially inward and positioned in

Figure 1 Gas phase composition in an (a) oxygen or (b) argon plasma: (■) without plasma, (▦) plasma without sample, and (▨) plasma with $C_{36}H_{74}$ (discharge conditions: 60 W, 40 $cm^3_{(STP)}$/min, and 0.30 torr).

the middle of the cover via an optical fiber. A 0.2-m Jobin-Yvon monochromator (HR 320) equipped with a PM R446 photomultiplier tube (PMT) was used to measure the emission intensity with a resolution of 0.4 Å at 5460 Å. The whole process is monitored by a Spectralink and analyzed by a computer. The spectra systems of these emission lines were reported elsewhere.[15-18]

Materials

The solvents used were distilled twice under argon on sodium wire. $C_{36}H_{74}$ (98% pure) was purchased

Table I Fragmentation Pattern of the Relevant Molecules in This Study

m/z	1	2	12	14	16	17	18	20	28	32	40	44
H_2	2.0	98.0	—	—	—	—	—	—	—	—	—	—
Ar	—	—	—	—	—	—	—	14.5	—	—	85.5	—
O_2	—	—	—	—	9.9	—	—	—	—	90.1	—	—
CO	—	—	4.6	0.9	0.9	—	—	—	92.6	—	—	—
H_2O	—	0.8	—	—	0.8	18.4	80	—	—	—	—	—
CO_2	—	—	4.7	—	7.1	—	—	—	8.7	—	—	78.7

from Aldrich and recrystallized from a hexane solution. OOD was synthesized by reacting at 90°C octadecanol with octadecanoylchloride in $CHCl_3$, with triethylamine used as HCl trap. The ester was then purified by chromatography on a silica gel column and recrystallized from acetone.

$C_{36}H_{74}$ and OOD films were prepared by slow evaporation under argon-reduced pressure on aluminum sheets (35 cm^2) of a benzene or acetone solution, respectively. Their crystals are known as rhombic lozenge-shape tablets. The surface morphology of the films prepared have been described elsewhere.[14]

RESULTS AND DISCUSSION

Gas Flow Rate Influence

Degradation

The gas flow rate influence was studied by keeping the other parameters constant (power: 60 W, pressure: 0.30 torr), and the flow rate was varied from 10 to 60 cm$^3_{(STP)}$/min. Figure 2 shows the evolution of the etching rate of $C_{36}H_{74}$ and OOD treated in an oxygen or argon plasma versus gas flow rate. The etching rate of both samples increases rapidly with oxygen flow rate from 10 to 30 cm$^3_{(STP)}$/min and reaches a plateau around 50 cm$^3_{(STP)}$/min. Just as it was observed in the study of power influence, the etching rate of OOD is always higher than that of $C_{36}H_{74}$. The fact that these two curves are parallel indicates that the ester group influence does not change with gas flow rate. In the case of an argon plasma, the gas flow rate has no effect on degradation, and the difference between $C_{36}H_{74}$ and OOD is very small.

Mass Spectrometry

The composition of the volatile phase coming from degradation is analyzed by mass spectrometry. The influence of oxygen flow rate on the concentration

of CO_2, CO, H_2O, and H_2 is shown in Figure 3(a_1) and 3(a_2) for $C_{36}H_{74}$ and OOD, respectively. In the case of $C_{36}H_{74}$, the concentrations of H_2O and CO increase rapidly with oxygen flow rate, reach a maximum value at around 20 cm$^3_{(STP)}$/min then decrease; the evolution of those of H_2 and CO_2 is comparable though less abrupt. In the case of OOD, the evolution of [CO] and [CO_2] is equivalent to that observed in $C_{36}H_{74}$, whereas [H_2] decreases almost linearly with the increase of oxygen flow rate, and [H_2O] stays nearly constant from 10 to 40 cm$^3_{(STP)}$/min and then decreases.

In the case of an argon plasma [Fig. 3(b)], [H_2] and [CO] decrease almost linearly with flow rate for both $C_{36}H_{74}$ and OOD. Just as the degradation rate, the difference of their concentrations between the two samples is too small to be considered.

The variation of the gas phase composition with gas flow rate is consistent with the degradation rates. The concentration of the degradation products results from the balance between their formation by
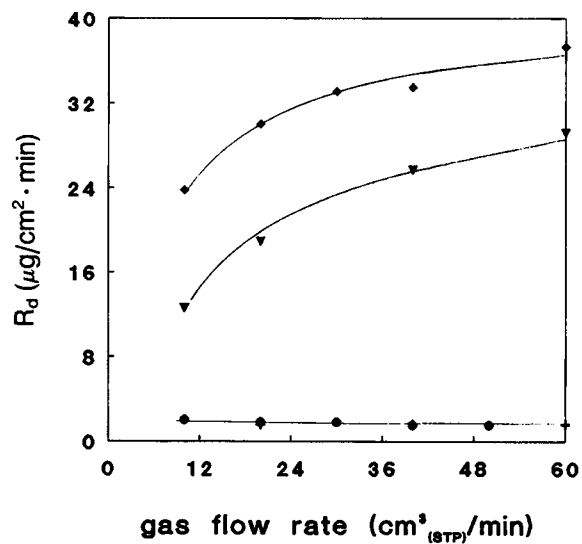

Figure 2 Degradation rates versus gas flow rate at 60 W, 0.30 torr. (♦) OOD–O_2, (▼) $C_{36}H_{74}$–O_2, (●) OOD–Ar, (+) $C_{36}H_{74}$–Ar.
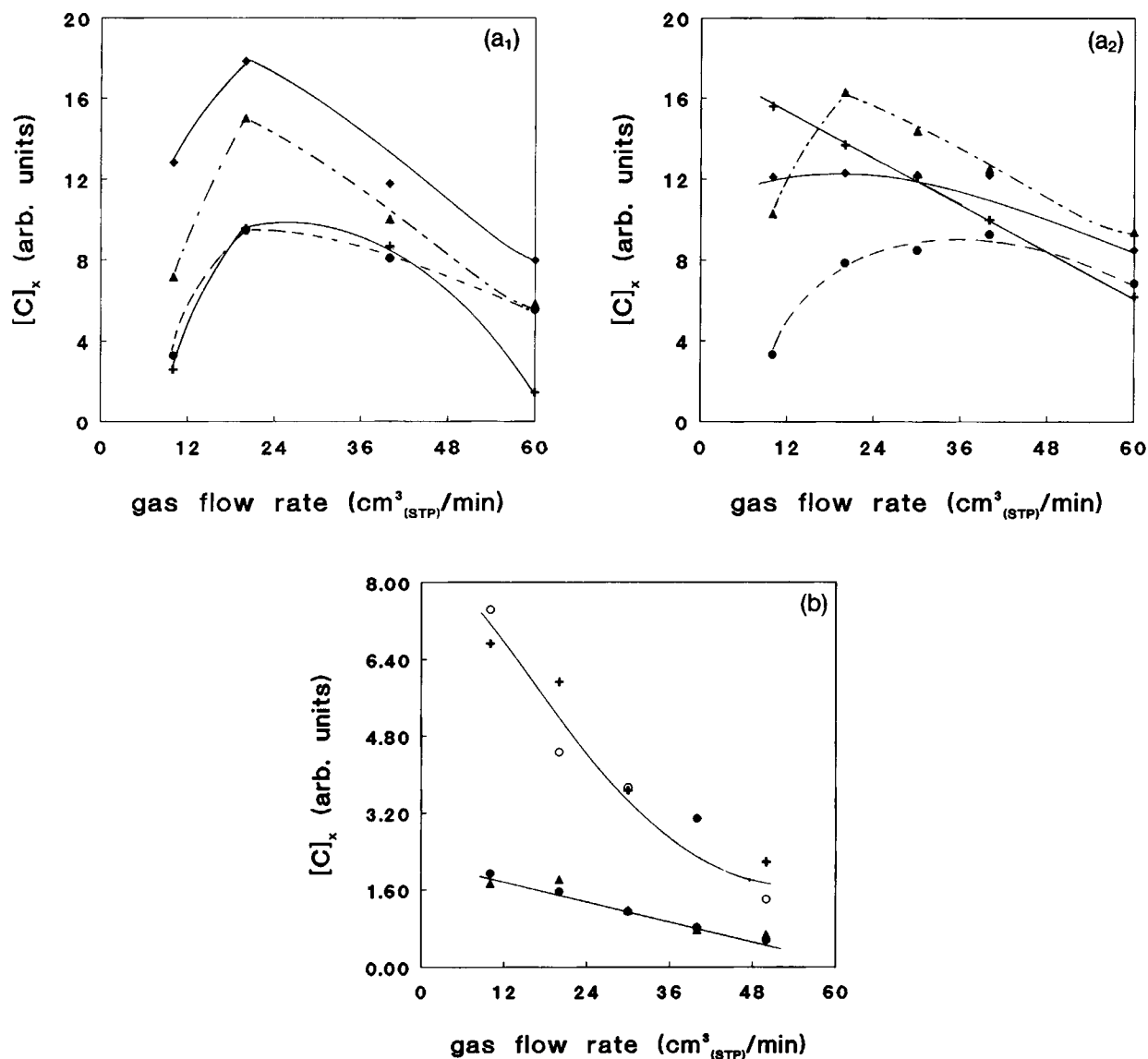
Figure 3 Concentration of the degradation products versus gas flow rate at 60 W, 0.30 torr in an (a) oxygen plasma for (a₁) $C_{36}H_{74}$ and (a₂) OOD. (◆) [H_2O], (▲) [CO], (+) [H_2], (●) [CO_2]; (b) argon plasma: (○) [H_2]–OOD, (+) [H_2]–$C_{36}H_{74}$, (▲) [CO]–OOD, (●) [CO]–$C_{36}H_{74}$.

degradation reactions and their elimination by gas flow; both processes increase with gas flow rate.

In an oxygen plasma, at low flow rate, the residence time is high, and the accumulation of these products formed continuously from degradation predominates, whereas at high flow rate, the elimination prevails. Of course, the competition between accumulation and elimination depends on the etching rates, in other words the supply of the volatile compounds. If this latter is not sufficient, the elimination would become dominant. This is what was observed in an argon plasma.

Optical Emission Spectroscopy

Optical emission spectroscopy provides us with an *in situ* measurement of the emission intensity in the glow discharge. In this study, the evolution of emission intensities of O-atoms (I_O at 7772 Å), CO (I_{CO} at 2833 Å), CO_2 (I_{CO2} at 2883 Å), and Hα (I_{Ha} at 6563 Å) in an oxygen plasma and those of Ar (I_{Ar} at 7504 Å), Hα, CO, and CH (I_{CH} at 4315 Å)) in an argon plasma has been investigated. The dependence of their emission intensities on the treatment time and the applied power was studied earlier.[14]

In an oxygen plasma, the variation of I_O with flow rate is shown in Figure 4(a). It is observed that without a sample, I_O decreases very slightly with increasing flow rate. But when a sample ($C_{36}H_{74}$ or OOD) is present, its variation is completely different: first, it increases with oxygen flow rate, becomes higher than the background value from 25 $cm^3_{(STP)}$/min; reaches a maximum value at around

30 $cm^3_{(STP)}$/min, and then decreases as when there is no sample. The difference of I_O between two samples $C_{36}H_{74}$ and OOD is not significant. The evolution of the emission intensities of the degradation products with flow rate are reported in Figure 4(a) and 4(b), respectively. As can be seen, I_{Ha} and I_{CO2}, just as $[H_2]$ and $[CO_2]$ detected by mass spectrometry, exhibit also a maximum value, but the position
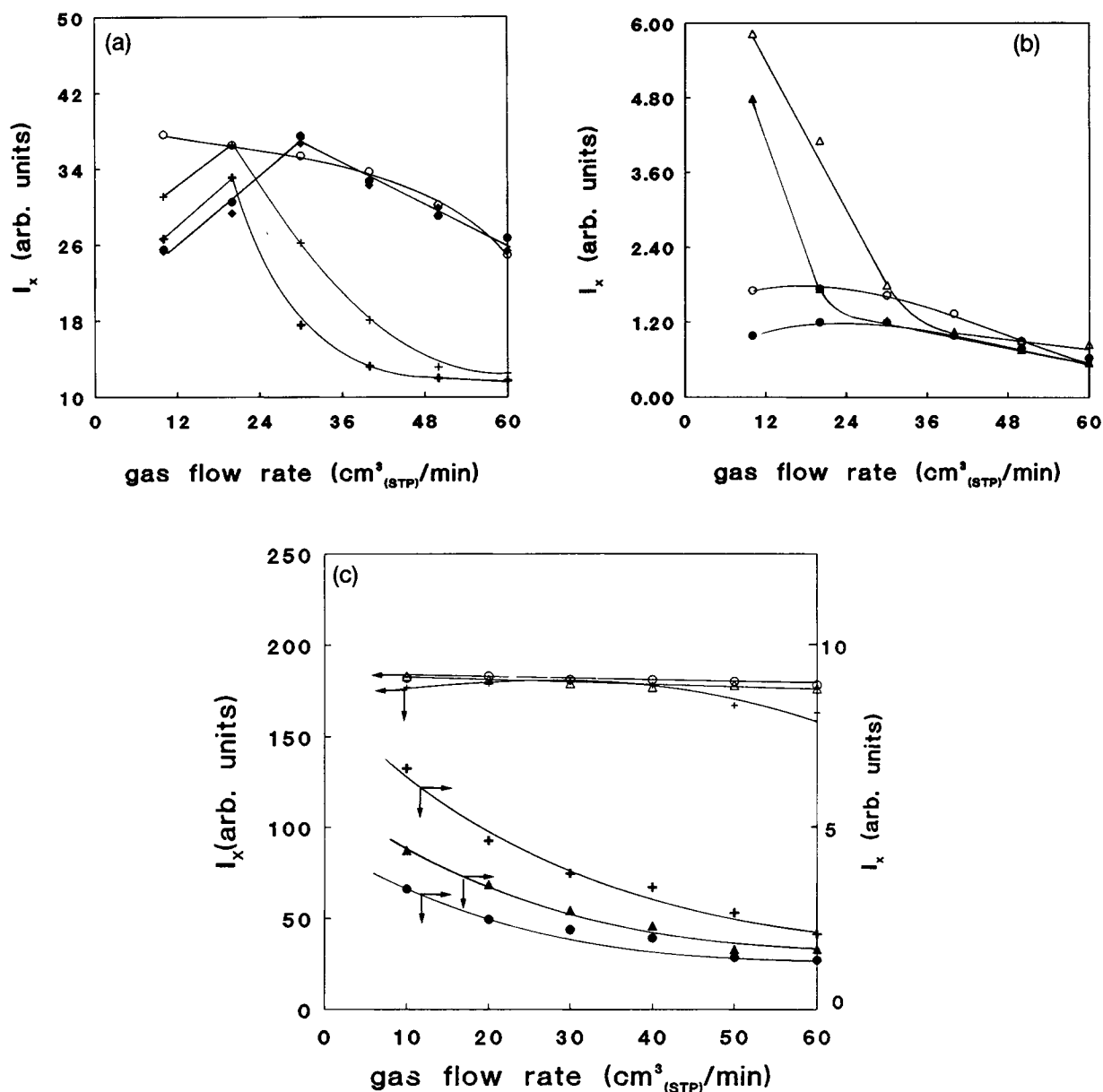

Figure 4 Evolution of the emission intensity versus gas flow rate in an oxygen plasma at 60 W, 0.30 Torr. (a) (O) I_O–without sample, (●) I_O–$C_{36}H_{74}$, (♦) I_O–OOD, (+) I_{Ha}–OOD, (+) I_{Ha}–$C_{36}H_{74}$. (b) (△) I_{CO}–OOD, (▲) I_{CO}–$C_{36}H_{74}$, (○) I_{CO2}–OOD, (●) I_{CO2}–$C_{36}H_{74}$. (c) An argon plasma at 60 W, 0.30 torr: (△) I_{Ar}–OOD, (○) I_{Ar}–$C_{36}H_{74}$, (+) I_{Ar}–without sample, (+) I_{Ha}–$C_{36}H_{74}$, (▲) I_{CO}–$C_{36}H_{74}$, (●) I_{CH}–$C_{36}H_{74}$.

is reached earlier for degradation products than that reached for oxygen atom emission intensity. The emission intensity of CO diminishes in all the range explored. The values of I_{Ha}, I_{CO}, and I_{CO2} are always higher for OOD than for $C_{36}H_{74}$, in agreement with the etching rate.

In an argon plasma [Fig. 4(c)], the emission intensity of Ar (7504 Å) without a sample decreases slightly with increasing gas flow rate. Opposite to that observed in an oxygen plasma, I_{Ar} with a sample is always slightly lower than that without a sample. The intensity difference of the degradation products between $C_{36}H_{74}$ and OOD is too small to be considered, only those of $C_{36}H_{74}$ are shown in Figure 4(c). All of them, I_{Ha}, I_{CO}, and I_{CH}, decrease monotonously with increasing flow rate. As the degradation rate does not depend on flow rate, this behavior can be attributed only to the decrease of their residence time in the reactor.

In the case of an argon plasma, due to its unreactive nature, degradation is produced essentially by the bombardment of argon atoms and ions. Therefore, the etching rate is determined only by the energy of the incident species. The fact that the flow rate has no effect on the etch rate means that the variation of the electron energy and its density is not important.

In the case of an oxygen plasma, up to 30 $cm^3_{(STP)}$/min, the degradation rate and the atomic oxygen emission intensity increase together. Generally, the degradation in an oxygen plasma is attributed to atomic oxygen and ion bombardement. The atomic oxygen concentration depends on:

1. The dissociation of O_2 through electron bombardment. It varies with the electron energy and its density, which should be independent of the gas flow rate since the pressure and the power are constant.
2. The presence of a dielectric on the grounded electrode, which can decrease the electronic density; however, this effect should be independent of the gas flow rate because the sample surface stays constant.
3. Its enhancement by the involvement of the degradation products such as OH, H_2, and H_2O in the formation of atomic oxygen.[19,20]
4. Its consumption by surface reactions. This phenomenon can explain the smaller emission intensity at lower flow rate when a sample is present. But the emission intensity should continue to decrease when the gas flow rate increases because of the rise in degradation rate.

By emission spectroscopy, only the excited part of the atomic oxygen is detected. By comparing the evolution of the oxygen atomic emission with and without a sample, it appears when a sample is present that:

1. At low flow rate, the concentration of the degradation products is low; the loss of atomic oxygen by the second and forth points is higher than its production by the third one.
2. At higher flow rate, because of the increase of the degradation rate, the formation of atomic oxygen increases faster than its loss until the residence time is so short that the degradation products are eliminated too fast to make the effect of their involvement important.

The degradation rate does not follow the apparent evolution of atomic oxygen emission. It continues to increase beyond 30 $cm^3_{(STP)}$/min although much more slowly. To explain this behavior, it should be taken into account that:

1. Both the surface and the gas phase recombination reactions diminish with increasing flow rate, resulting in a relative increase of the atomic flux at the surface.[14]
2. The residence time of all of the species diminishes with increasing gas flow rate, inducing more efficiently the removal of the active species such as OH·[3] and the shift of the
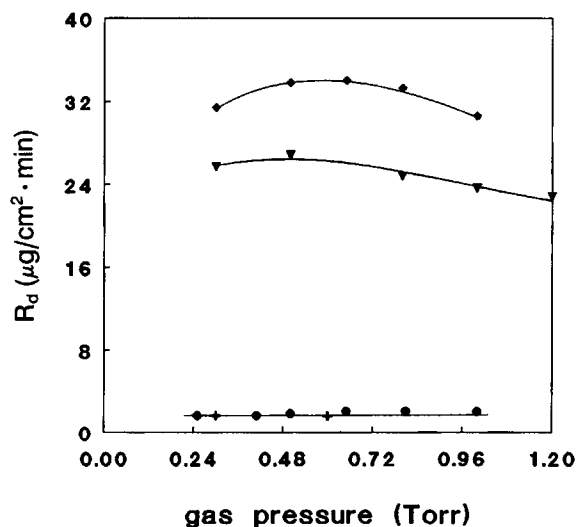

Figure 5 Degradation rates versus gas pressure at 60 W, 40 $cm^3_{(STP)}$/min. (♦) OOD–O_2, (▼) $C_{36}H_{74}$–O_2, (●) OOD–Ar, (+) $C_{36}H_{74}$–Ar.

steady state, which speeds up the formation of the products and thereby the degradation.

In the case of an argon plasma, there is no involvement of the degradation products in the formation of excited species. The emission intensity decreases monotonously though slightly with increasing gas flow rate although the degradation rate is virtually unchanged.

From the above discussion, it can be concluded: Gas flow rate is an important parameter that should be taken into account in the study of the treatment processes. It is directly related to the composition of the plasma gas phase and determines the diffusion of the reactives species to the reaction sites. A quantitative measurement of the atomic oxygen at surface level is absolutely necessary to confirm this hypothesis.
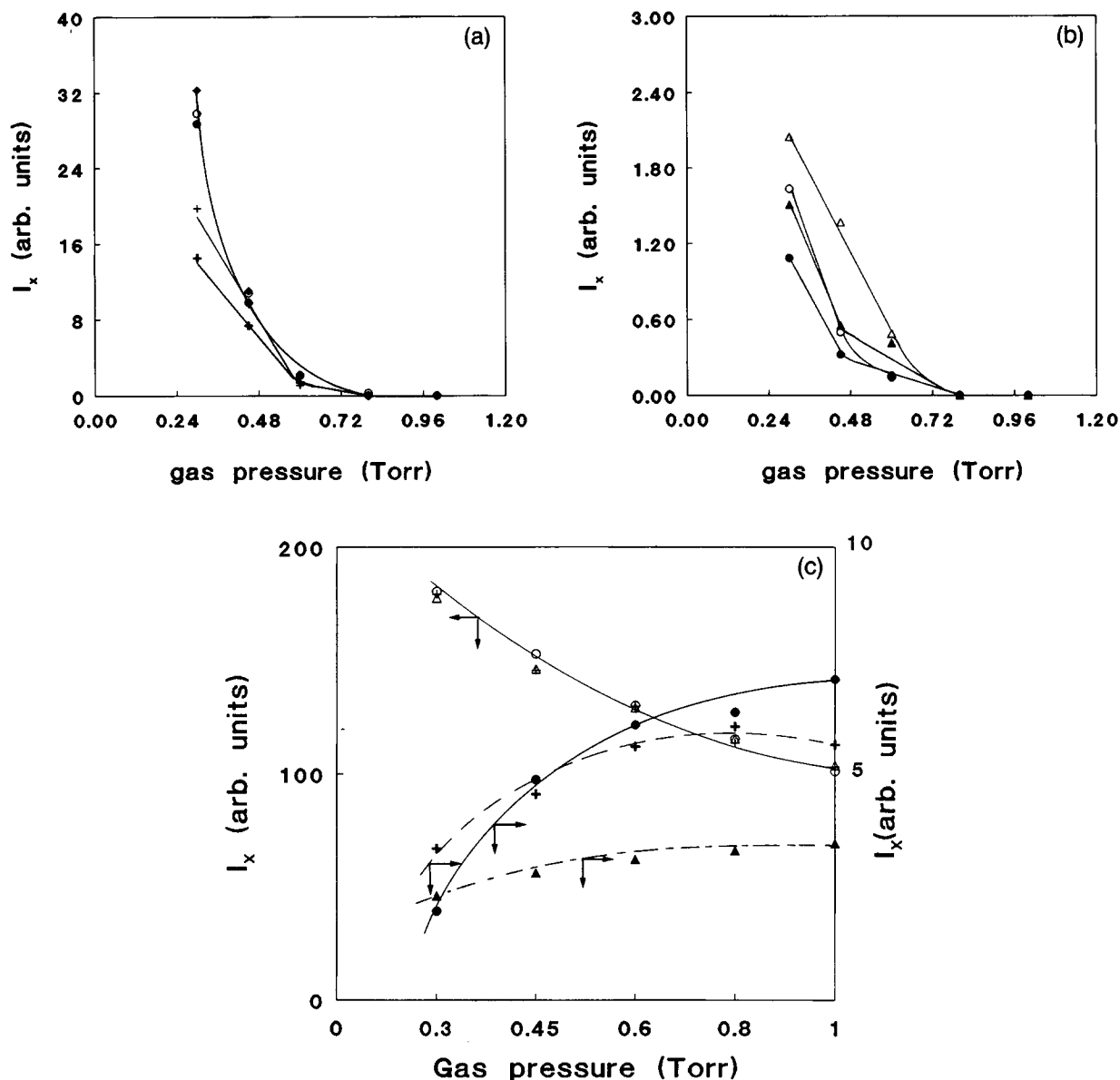

Figure 6 Evolution of the emission intensity versus gas pressure in (a) an oxygen plasma at 60 W, 40 $cm^3_{(STP)}$/min. (○) I_O–$C_{36}H_{74}$; (◆) I_O–OOD, (●) I_O–without sample, (+) I_{Ha}–$C_{36}H_{74}$; (b) an oxygen plasma at 60 W, 40 $cm^3_{(STP)}$/min. (△) I_{CO}–OOD, (▲) I_{CO}–$C_{36}H_{74}$, (○) I_{CO2}–OOD, (●) I_{CO2}–$C_{36}H_{74}$; (c) an argon plasma at 60 W, 40 $cm^3_{(STP)}$/min. (△) I_{Ar}–OOD, (○) I_{Ar}–$C_{36}H_{74}$, (+) I_{Ar}–without sample, (+) I_{Ha}–$C_{36}H_{74}$, (▲) I_{CO}–$C_{36}H_{74}$, (●) I_{CH}–$C_{36}H_{74}$.

Pressure Influence

Reactions were carried out at constant power and gas flow rate equal, respectively, to 60 W and 40 $cm^3_{(STP)}$/min.

Degradation

The influence of the gas pressure on degradation is reported in Figure 5. It is observed that in the case of an oxygen plasma, the rate of weight loss increases slightly to a maximum before decreasing. But these variations are very small as compared to the absolute values. Again, the etching rate of OOD is always higher than that of $C_{36}H_{74}$, and the effect of ester
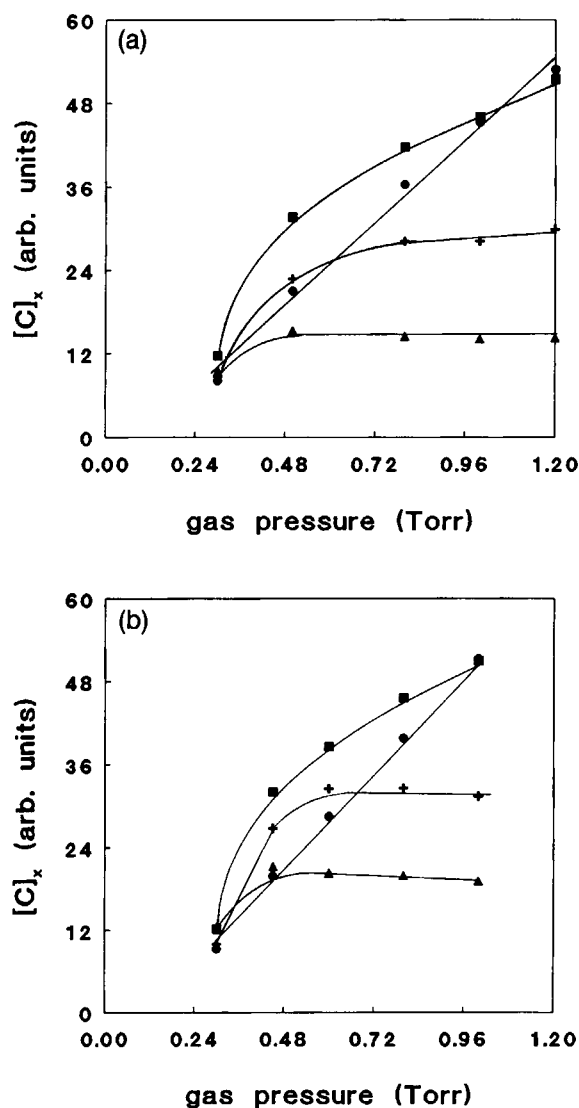
Figure 7   Concentration of the degradation products versus gas pressure at 60 W, 40 $cm^3_{(STP)}$/min in an oxygen plasma for (a) $C_{36}H_{74}$ and (b) OOD. (■) [H_2O], (▲) [CO], (+) [H_2], (●) [CO_2].
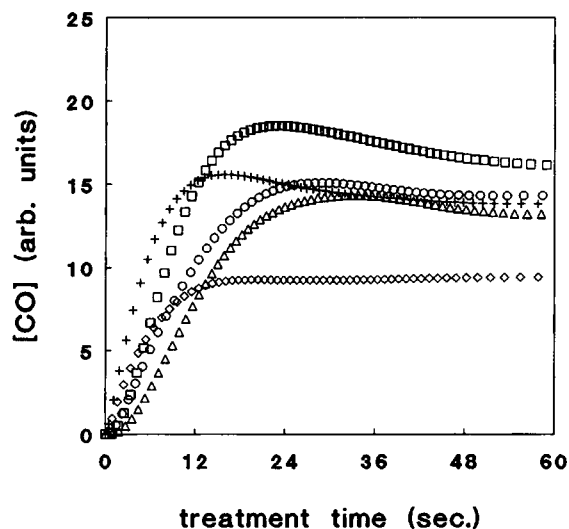
Figure 8   Variation of the CO concentration versus gas pressure at 60 W, 40 $cm^3_{(STP)}$/min in an oxygen plasma. (◇) 0.30 torr, (+) 0.50 torr, (□) 0.65 torr, (○) 0.80 torr, (△) 1.00 torr.

groups on OOD seems to be independent of the pressure. No effect can be observed in an argon plasma.

It was observed[12] that while the electron energy decreases (hence the average energy of the reactive particles) with increasing pressure, its density increases. The degradation behavior observed is probably a result of these two antagonist effects.

Optical Emission Spectroscopy

Opposite to the degradation behavior, the intensity of all the emission lines decreases sharply with pressure in an oxygen plasma and becomes equal to zero after 0.80 torr [Figs. 6(a) and 6(b)]. Invisible because of the drop in intensity, the difference of I_O with or without sample is difficult to estimate. But I_{Ha}, I_{CO}, and I_{CO2} are higher for OOD than for $C_{36}H_{74}$; the difference between them can be observed only at low pressure.

In the case of an argon plasma [Fig. 6(c)], I_{Ar} decreases also rapidly with increasing pressure, but I_{CO}, I_{CH}, and I_{Ha} increase. As the rate of weight loss does not depend on pressure, this important increase must be due to their accumulation in the reactor. This is confirmed by the subsequent study of mass spectrometry.

It should be noted that by optical emission spectroscopy, one measures the concentration of the species that are in their excited states. The decrease of the emission intensity is partly due to the decrease in electron energy, which induces a decrease in the excitation process by electron bombardment, and

partly to the "quenching effect" that results in the deactivation of the excited particles through inelastic collisions with other species. Indeed, as the mean free path of the particles decreases with increasing pressure, the number of inelastic collisions increases. It appears that an oxygen plasma is much more sensitive to the quenching effect than an argon plasma.

Mass Spectrometry

The variation of the degradation products as a function of oxygen pressure is reported in Figures 7(a) and 7(b) for $C_{36}H_{74}$ and OOD, respectively. It is

observed that $[CO_2]$ increases almost linearly with pressure; $[H_2O]$ increases even more rapidly than $[CO_2]$ from 0.30 to 0.8 torr, then reaches a plateau; $[CO]$ and $[H_2]$ reach quickly a plateau at about 0.50 torr. It should be noted that there is a change of the relative concentration with pressure: $[CO_2]$, which is slightly smaller than $[CO]$ at 0.3 torr, increases very rapidly with pressure. Its evolution is exactly the same for $C_{36}H_{74}$ and OOD. Because the degradation is slightly dependent on pressure, these phenomena can be attributed to the accumulation of these products in the reactor. At constant gas flow rate, the linear velocity of gas flow is inversely pro-
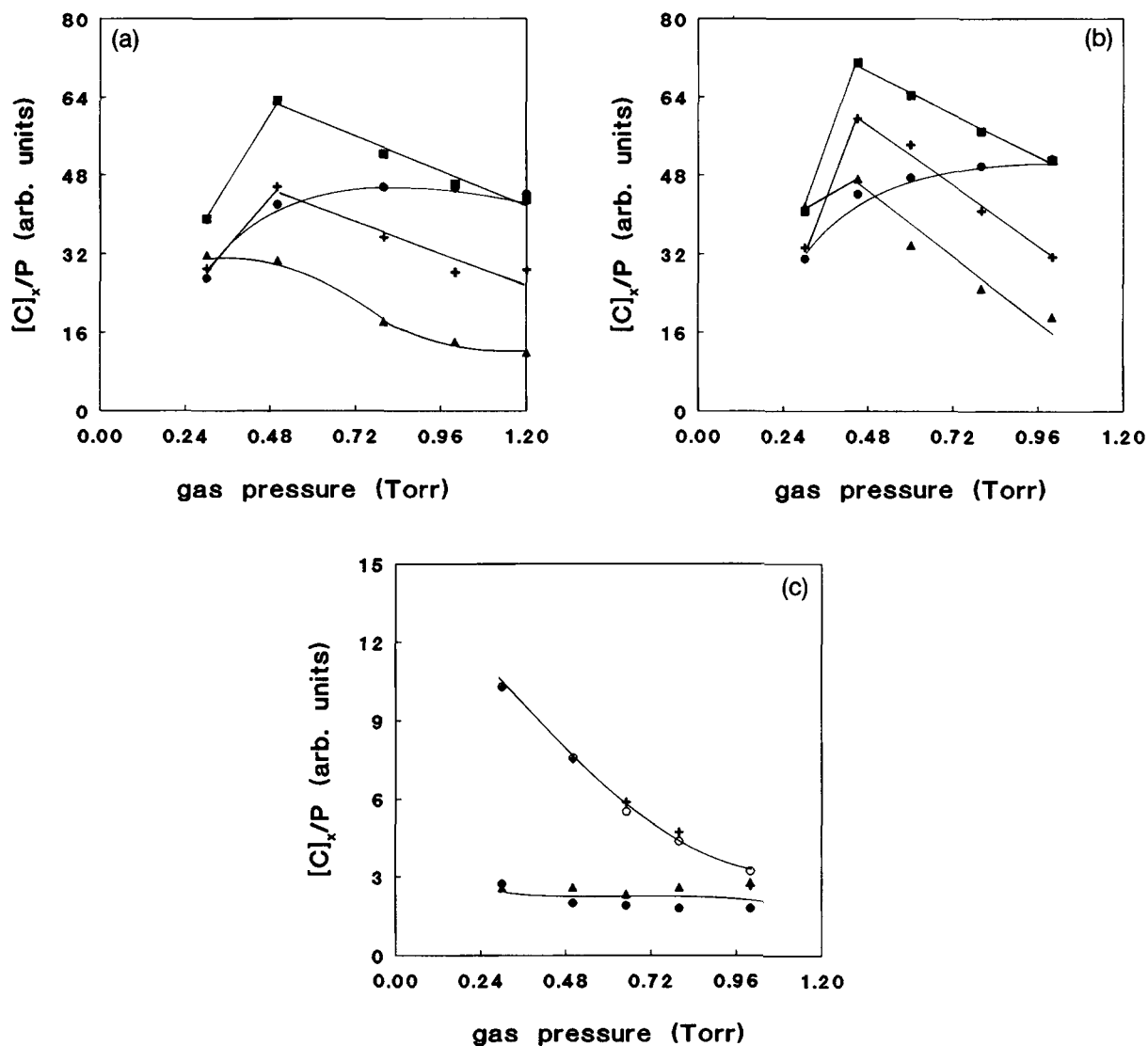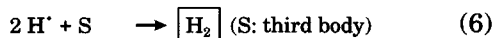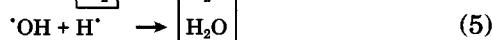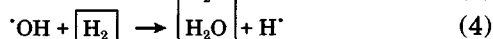

Figure 9 Corrected concentration of the degradation products versus gas pressure at 60 W, 40 $cm^3_{(STP)}$/min in an oxygen plasma for (a) $C_{36}H_{74}$ and (b) OOD. (■) $[H_2O]$, (▲) $[CO]$, (+) $[H_2]$, (●) $[CO_2]$; and (c) corrected concentration of the degradation products versus pressure in an argon plasma at 60 W, 40 $cm^3_{(STP)}$/min. (○) $[H_2]-C_{36}H_{74}$, (+) $[H_2]-$ OOD, (●) $[CO]-C_{36}H_{74}$, (▲) $[CO]-OOD$.

portional to pressure. Thus the higher the pressure, the more important the accumulation effect. This is clearly shown in Figure 8, in which the time necessary to reach a steady [CO] increases progressively with pressure.

To take into account this accumulation effect, the concentration of the degradation products was divided by their corresponding pressure; the results were plotted versus pressure and shown in Figures 9(a) and 9(b). Except for [CO], which decreases in the whole range, [H_2O], [H_2], and [CO_2] all show a maximum value at around 0.5 torr, in accordance with the evolution of the degradation rates.

The same accumulation behavior is observed in an argon plasma, but it is much less important as compared to that observed in an oxygen plasma mainly due to the smaller degradation rate; therefore after division by the corresponding pressure, the concentration of the degradation products decreases monotonously with increasing pressure [Fig. 9(c)].

The accumulation is an important factor but cannot be the only effect of increasing pressure, because the relative concentration of the degradation products change with pressure while the rate of their formation by degradation is almost constant. In other words if, indeed, the accumulation is the only effect brought about by increasing pressure, the same variation of these effluents versus pressure should have been observed. The chemical reactions that take place in the gas phase should be taken into account to explain their evolution. The reactions that should be considered are as follows:

$$\boxed{CO} + {}^{\bullet}OH \rightarrow \boxed{CO_2} + H^{\bullet} \qquad (1)$$
$$\boxed{CO} + O \rightarrow \boxed{CO_2} \qquad (2)$$

$${}^{\bullet}OH + RH \rightarrow \boxed{H_2O} + R^{\bullet} \qquad (3)$$
$${}^{\bullet}OH + \boxed{H_2} \rightarrow \boxed{H_2O} + H^{\bullet} \qquad (4)$$
$${}^{\bullet}OH + H^{\bullet} \rightarrow \boxed{H_2O} \qquad (5)$$

$$2\,H^{\bullet} + S \rightarrow \boxed{H_2} \quad (S: \text{third body}) \qquad (6)$$
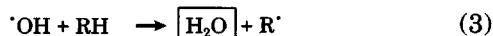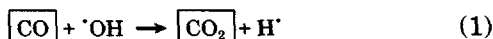
When the pressure increases, the concentration of O atoms, OH and H$^{\bullet}$ radicals increase, thus favoring the formation of CO_2 and H_2O to the detriment of CO and H_2. This is confirmed by the following study of the gas composition influence.

Gas Composition Influence

The influence of gas mixtures (Ar + O_2) and (N_2 + O_2) on the degradation rates of $C_{36}H_{74}$ was investigated in the following conditions: power, 60 W;

pressure, 0.30 torr; total gas flow rate, 40 $cm^3_{(STP)}$/min, and treatment time 10 min. First, we checked that the rate of degradation increases linearly with the treatment time; then the degradation rates were calculated.

Degradation

The etching rate of $C_{36}H_{74}$ as a function of oxygen percentage $O_2\%$ is shown in Figure 10. The oxygen percentage is given as $100 * [O_2]/([O_2] + [X])$ (X = Ar or N_2); their concentrations are detected by mass spectrometry. It is observed that the etching rate increases almost linearly with $O_2\%$ when this latter is lower than 60 and reaches a maximum at about 80 then decreases slightly. The mixture of (Ar + O_2) is slightly more reactive than that of (N_2 + O_2), but these two curves are very similar and the difference between them is very small.

N_2 is known as a reactant that can enhance the O-atom concentration.[19] Premachandran[11] reported that the etching rate of photoresist was greatly enhanced by adding only 1% of N_2 into the oxygen plasma.

Mass Spectrometry

The concentration of CO in the mixture of (N_2 + O_2) is not shown because the m/z value for N_2 and CO is the same and the concentration of N_2 is so high as to make insignificant the variation of the peak at 28. The concentration of the degradation products
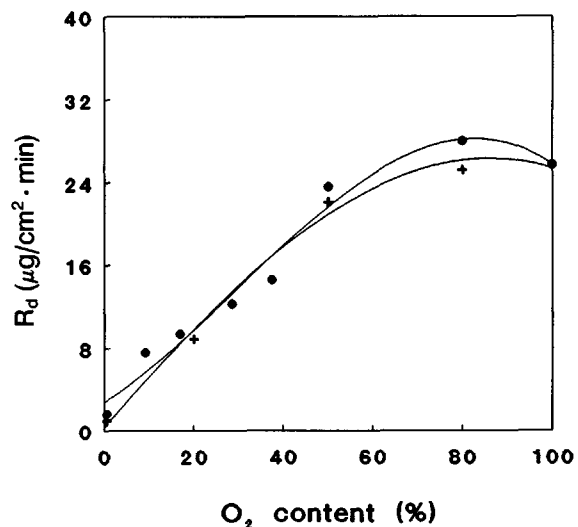

Figure 10 $C_{36}H_{74}$ degradation rate versus oxygen content (%) in (●) (Ar + O_2) and (+) (N_2 + O_2) discharges at 60 W, 0.30 torr for a total gas flow of 40 $cm^3_{(STP)}$/min.

in the gas phase increases with the oxygen content in agreement with the degradation rate in the mixture $(Ar + O_2)$ as in $(N_2 + O_2)$ [Fig. 11(a) and 11(b)]. The concentration of H_2 and CO reaches a maximum at around 60% before decreasing, while the maximum of H_2O and CO_2 concentrations are reached at around 80%.

It should be pointed out that there is a change in the relative concentrations of the degradation products with increasing oxygen content. Until 50% of O_2, [CO] is widely higher than [CO_2], but after the increase of CO_2 becomes faster than that of CO so
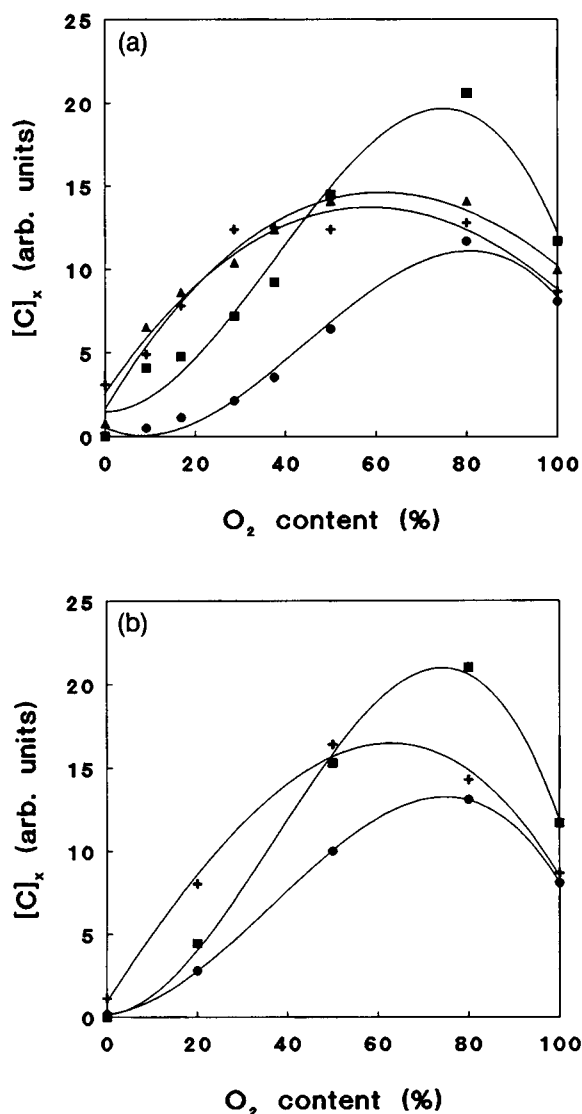
that at 80% of O_2, their concentration is equal. The same evolution is observed for H_2 and H_2O, but above 50%, H_2O is bigger than CO. As the pressure is kept constant, the accumulation effect should not be very different with O_2%. Thus the change of the relative concentrations can be attributed mainly, if not only, to the chemical reactions [Eqs. (1)–(5)]. At low oxygen content (<40%), the formation of CO_2 and H_2O is limited by O-atom supply, therefore [H_2O] and [CO_2] are lower than [H_2] and [CO]. But at higher oxygen rate, the supply of O atoms is sufficient to convert CO and H_2 to CO_2 and H_2O, respectively. The same effect was reported by Mogab et al.[21] who studied the etching of Si and SiO_2 by $(O_2 + CF_4)$ RF plasma by mass spectrometry. They observed that [CO_2] increases more importantly than [CO] and [COF_2] when O_2% is increased.

The emission properties of the mixture are not investigated because the nature of these two gases are completely different, which can induce an important change in electronic density.

CONCLUSION

This study has shown that the gas flow rate and pressure, by modifying the residence time, the electron energy, and its density, are very important parameters in the interaction of cold plasmas with polymer surfaces.

In terms of degradation rate, the difference between $C_{36}H_{74}$ and OOD surface does not depend on the pressure and on the gas flow rate.

The concentration of the degradation products in the gas phase is in good agreement with the degradation rates and are the result of the balance between their formation rate on the surface or in the gas phase reactions and their elimination by the gas flow.

The atomic oxygen emission seems to be directly dependent on the atomic oxygen consumption on the sample surface and the presence of the degradation products in the gas phase.

This study confirms the tight interdependance between the emission intensities of excited species and the concentrations of degradation products in the gas phase, which affects the reaction kinetics on the sample surface and in the gas phase.

Figure 11   Concentration of the degradation products versus oxygen content (%) (a) $(Ar + O_2)$, (■) [H_2O], (▲) [CO], (+) [H_2], (●) [CO_2]. (b) $(N_2 + O_2)$ discharges: (■) [H_2O], (+) [H_2], (●) [CO_2], operating conditions see Figure 10.

REFERENCES

1. R. H. Hansen, J. O. Pascale, T. D. Benedictis, and P. M. Rentzepis, *J. Polym. Sci., A*, **3**, 2205 (1965).

2. T. Yasuda, M. Gazicki, and H. Yasuda, *J. Appl. Polym. Sci. Appl. Polym. Symp.,* **38,** 201, (1984).

3. N. R. Lerner and T. Wydeven, *J. Appl. Polym. Sci.,* **35,** 1903, (1988).

4. H. Yasuda, C. E. Lamaze, and K. Sakaoku, *J. Appl. Polym. Sci.,* **17,** 137, (1973).

5. M. A. Hartney, W. M. Greene, D. S. Soane, and D. W. Hess, *J. Vac. Sci. Technol.,* **B6**(6), 1892, (1988).

6. M. A. Golub and T. Wydeven, *Polym. Deg. Stab.,* **22,** 325, (1988).

7. K. Harada, *J. Appl. Polym. Sci.,* **26,** 1961, (1981).

8. P. M. Scott, S. V. Babu, R. E. Partch, and L. J. Matiento, *Polym. Deg. Stab.,* **27,** 169, (1990).

9. T. Wydeven, M. A. Golub, and N. R. Lerner, *J. Appl. Polym. Sci.,* **37,** 3343, (1989).

10. S. Dzioba, G. Este, and H. M. Naguib, *J. Electrochem.,* **189,** 2537, (1982).

11. V. Premachandran, *Appl. Phys. Lett.,* **52,** 2488, (1989).

12. G. R. Misium, *J. Vac. Sci. Technol.,* **A(8),** 1642, (1990).

13. M. Dalvie and K. F. Jensen, *J. Vac. Sci. Technol.,* **A(8),** 1648, (1990).

14. F. Clouet and M. K. Shi, *J. Appl. Polym. Sci.,* to appear.

15. R. d'Agostino, F. Cramarossa, S. D. Benedictis, and G. Ferraro, *J. Appl. Phys.,* **52,** 1259, (1981).

16. A. D. Kuypers, A. Koch, and H. J. Hopman, *J. Vac. Sci. Technol.,* **A(8),** 3736, (1990).

17. R. E. Walkup, K. L. Saenger, and G. S. Selwyn, *J. Chem. Phys.,* **84**(5), 2668, (1986).

18. T. Kokubo, F. Tochikubo, and T. Makabe, *Appl. Phys. Lett.,* **56,** 818, (1990).

19. F. Kaufmann and J. R. Kelso, *J. Chem. Phys.,* **32,** 301, (1960).

20. F. Kaufmann, *Adv. Chem. Series,* **80,** 29, (1969).

21. C. J. Mogab, A. C. Adams, and D. L. Flamm, *J. Appl. Phys.,* **49**(7), 3796, (1978).